



Deposited via The University of Sheffield.

White Rose Research Online URL for this paper:

<https://eprints.whiterose.ac.uk/id/eprint/185785/>

Version: Accepted Version

Article:

Chen, H., Jiang, Z., Liu, W. et al. (2022) Conjugate augmented decoupled 3-D parameters estimation method for near-field sources. *IEEE Transactions on Aerospace and Electronic Systems*, 58 (5). pp. 4681-4689. ISSN: 0018-9251

<https://doi.org/10.1109/taes.2022.3164864>

© 2022 IEEE. Personal use of this material is permitted. Permission from IEEE must be obtained for all other users, including reprinting/ republishing this material for advertising or promotional purposes, creating new collective works for resale or redistribution to servers or lists, or reuse of any copyrighted components of this work in other works. Reproduced in accordance with the publisher's self-archiving policy.

Reuse

Items deposited in White Rose Research Online are protected by copyright, with all rights reserved unless indicated otherwise. They may be downloaded and/or printed for private study, or other acts as permitted by national copyright laws. The publisher or other rights holders may allow further reproduction and re-use of the full text version. This is indicated by the licence information on the White Rose Research Online record for the item.

Takedown

If you consider content in White Rose Research Online to be in breach of UK law, please notify us by emailing eprints@whiterose.ac.uk including the URL of the record and the reason for the withdrawal request.



Conjugate Augmented Decoupled 3-D Parameters Estimation Method for Near-Field Sources

Hua Chen, *Member, IEEE*, Zhiwei Jiang, Wei Liu, *Senior Member, IEEE*,
Ye Tian, *Member, IEEE* and Gang Wang, *Senior Member, IEEE*

Abstract—A near-field (NF) source localization method is proposed for two-dimensional (2-D) direction-of-arrival (DOA) and range estimation based on a symmetrical cross array. It first employs the conjugate symmetry property of signal autocorrelation for different time delays to construct a conjugate augmented spatial-temporal cross correlation matrix, then the extended steering vector is decoupled to avoid the usual multi-dimensional (M-D) search based on the properties of the Khatri-Rao product, and finally three one-dimensional (1-D) MUSIC type searches are employed to obtain the results. The proposed method can realize automatic pairing of multiple parameters associated with each source and it also works in the underdetermined case. Furthermore, the stochastic Cramer-Rao lower bound (CRB) with different time delays is derived. Compared with two existing methods, simulation results demonstrate that the proposed method provides satisfactory estimation performance for both the DOA and range parameters at low signal-to-noise ratio (SNR) and with a small number of snapshots.

Index Terms—Near-field, spatial-temporal, multiple-dimensionality decoupled, cross array, automatically paired

I. INTRODUCTION

Source localization has a wide range of applications such as radar, sonar and wireless communications [1–4]. According to the distance from sources to the array, they can be divided into near-field (NF) and far-field (FF) ones. In FF source localization, also known as direction of arrival (DOA) estimation, the plane wave assumption is normally adopted. For NF sources, their wavefront curvature cannot be ignored as they lie in the Fresnel area of the array aperture. Thus, the waveform of NF sources characterized by both the DOA and range parameters is depicted with a spherical curvature, which varies nonlinearly with the array position.

Many efforts have been devoted to localization of FF sources, such as the subspace based methods [5, 6] and the sparsity based methods [7, 8]. However, these high resolution DOA estimation methods are not directly applicable to the

case with NF sources, as the propagation delay of NF sources, utilizing Fresnel approximation [9], varies quadratically with respect to sensor locations. In [10], a passive DOA and range estimation method for NF sources based on the maximum likelihood (ML) approach is proposed, which has a high parameter estimation accuracy by constructing a highly non-linear cost function with multi-dimensional (M-D) search. In [11], an improved two-dimensional (2-D) MUSIC algorithm is introduced to estimate the DOA and range of NF sources, involving a 2-D search procedure. A clear drawback of the methods in [10, 11] is their high computational complexity, and furthermore, they suffer from the pairing problem in the presence of multiple NF sources. On the basis of NF 2-D MUSIC, a method based on polynomial rooting instead of searching for range and bearing estimation is derived in [12], which reduces the computational cost to a certain extent, but again suffering from the same pairing problem. Then, an oblique projection based MUSIC (OPMUSIC) algorithm is proposed in [13], requiring several 1-D searches with a relatively low complexity, and in [14], the number of required searches is reduced to one. Employing higher order statistics, a two stage-MUSIC (TSMUSIC) algorithm [15] is proposed by constructing two different matrices to estimate the DOA and range, respectively. But the complexity of TSMUSIC is high due to the cumulant elements involved in the process.

One common limitation for the above-mentioned methods is that they are only focused on the problem of 2-D parameter positioning for NF sources, namely azimuth and range. In the three-dimensional (3-D) NF source model, the estimated parameters include not only azimuth and range, but also elevation, thus leading to an even more complicated parameter pairing problem. Although several methods have been reported for localization of NF sources using the spherical coordinates system (azimuth, elevation, and range), they are only efficacious for overdetermined or single source estimation [16–18]. Moreover, two cumulant based localization methods are introduced for 3-D NF sources in [19, 20]. Although the algorithms proposed in [13, 15] can also be directly extended to 3-D NF source positioning, they require more array sensors than the number of sources.

In this paper, a conjugate augmented spatial-temporal localization method for NF sources¹ is proposed employing a cross array. We first use the spatial-temporal characteristics of the array received data and the conjugate symmetry property

This work was supported by the National Natural Science Foundation of China under grant 62001256, and by Key Laboratory of Intelligent Perception and Advanced Control of State Ethnic Affairs Commission under grant MD-IPAC-2019102, and by Zhejiang Provincial Natural Science Foundation of China under grant LR20F010001, and the UK Engineering and Physical Sciences Research Council (EPSRC) under grants EP/T517215/1 and EP/V009419/1. (Corresponding authors: Hua Chen, Ye Tian.)

Hua Chen, Zhiwei Jiang, Ye Tian and Gang Wang are with the Faculty of Electrical Engineering and Computer Science, Ningbo University, Ningbo 315211, China. (e-mail: dkchenhua0714@hotmail.com; tianfield@126.com; wanggang@nbu.edu.cn.)

Wei Liu is with the Department of Electronic and Electrical Engineering, University of Sheffield, Sheffield S1 3JD, UK. (e-mail: w.liu@sheffield.ac.uk).

¹Because an FF source can be considered as a special NF one when range r approaches ∞ , the proposed method can also be adapted to mixed NF and FF sources.

of signal autocorrelation to increase the degrees of freedoms (DOFs), and then use the properties of the Khatri-Rao product and the 1-D MUSIC algorithm to obtain the estimated angle or range. This method can realize automatic pairing of the estimated parameters, and more importantly, it can correctly retrieve the parameter information in the underdetermined case, i.e. when the number of sources is larger than or equal to the number of array sensors.

Notations: Matrices and vectors are denoted by boldfaced capital letters and lower-case letters, respectively. For an integer M , $[M]$ is defined as the set $\{-M, \dots, 0, \dots, M\}$. $|\cdot|$ denotes the absolute value of a scalar or cardinality of a set. The superscript $(\cdot)^T$, $(\cdot)^*$, $(\cdot)^H$ and $(\cdot)^{-1}$ stand for transpose, conjugate, conjugate transpose, and inverse, respectively. The notations $E\{\cdot\}$, $\delta(\cdot)$, \otimes , \odot , \mathbf{I}_D , \mathbf{J}_D represent the statistical expectation, Dirac function, Kronecker product, Khatri-Rao (KR) product, the $D \times D$ identity matrix, the $D \times D$ exchange matrix with ones on its antidiagonal and zeros elsewhere, respectively. $\text{diag}\{\mathbf{Z}\}$ represents diagonal elements of the matrix \mathbf{Z} . $\text{blkdiag}\{\mathbf{Z}_1, \mathbf{Z}_2\}$ represents a block diagonal matrix with diagonal entries \mathbf{Z}_1 and \mathbf{Z}_2 . $\text{tr}(\cdot)$, $\text{vec}(\cdot)$, and $\det[\cdot]$ denote the trace, vectorization and determinant of a matrix, respectively.

II. SIGNAL MODEL

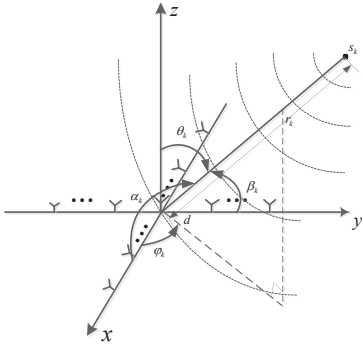


Fig. 1. 3-D localization configuration for NF sources.

As shown in Fig. 1, there are K NF, narrowband, spatially and temporally uncorrelated sources $\{s_k(n)\}_{k=1}^K$ ($n = 1, 2, \dots, N$, N denotes the number of snapshots) impinging onto a symmetric cross array consisting of two uniform linear arrays (ULAs). The ULA on x-axis is denoted as array \mathbf{x} , whose element indices are $[M_x] = \{-M_x, \dots, M_x\}$ and the total number of sensors is given by $N_x = |[M_x]|$. Similarly, the ULA on y-axis is represented as array \mathbf{y} , whose indices are denoted as $[M_y] = \{-M_y, \dots, M_y\}$ and its number of sensors is $N_y = |[M_y]|$. The element spacing of each array is d ($d \leq \lambda/4$, where λ denotes signal wavelength). In Fig. 1, let θ_k and φ_k denote the elevation and azimuth angles of the k -th signal, respectively, and α_k and β_k denote the angles between the k -th signal and the \mathbf{x} and \mathbf{y} axes, respectively. If α_k and β_k are determined, θ_k and φ_k can be uniquely identified. Let the array center be the phase reference point, the signals received by the two ULAs can be expressed

as:

$$x_m(n) = \sum_{k=1}^K s_k(n) e^{-j\tau_{m_x,k}} + n_{m_x}(n) \quad (1)$$

$$y_m(n) = \sum_{k=1}^K s_k(n) e^{-j\tau_{m_y,k}} + n_{m_y}(n) \quad (2)$$

where $x_m(n)$ and $y_m(n)$ are the received signals of the m -th sensor of array \mathbf{x} and array \mathbf{y} , respectively, $\tau_{m_x,k}$ and $\tau_{m_y,k}$ are the phase delays of the k -th signal to the m -th sensor of array \mathbf{x} and array \mathbf{y} , respectively, $n_{m_x}(n)$ and $n_{m_y}(n)$ are the corresponding Gaussian noises. With the Fresnel approximation in [20], $\tau_{m_x,k}$ and $\tau_{m_y,k}$ can be expressed as,

$$\tau_{m_x,k} = \omega_{xk}m + \phi_{xk}m^2 \quad (3)$$

$$\tau_{m_y,k} = \omega_{yk}m + \phi_{yk}m^2 \quad (4)$$

where

$$\omega_{xk} = -\frac{2\pi d}{\lambda} \cos \alpha_k, \phi_{xk} = \frac{\pi d^2}{\lambda r_k} \sin^2 \alpha_k \quad (5)$$

$$\omega_{yk} = -\frac{2\pi d}{\lambda} \cos \beta_k, \phi_{yk} = \frac{\pi d^2}{\lambda r_k} \sin^2 \beta_k.$$

Further, (1) and (2) can be written in a more compact form as follows,

$$\mathbf{x}(n) = \mathbf{A}_x \mathbf{s}(n) + \mathbf{n}_x(n) \quad (6)$$

$$\mathbf{y}(n) = \mathbf{A}_y \mathbf{s}(n) + \mathbf{n}_y(n), \quad (7)$$

where $\mathbf{x}(n)$ and $\mathbf{y}(n)$ denote the output vectors of array \mathbf{x} and array \mathbf{y} , respectively, $\mathbf{A}_x = [\mathbf{a}(\omega_{x1}, \phi_{x1}), \dots, \mathbf{a}(\omega_{xk}, \phi_{xk})]$ with $\mathbf{a}(\omega_{xk}, \phi_{xk}) = [e^{-j[\omega_{xk}(-M_x) + \phi_{xk}(-M_x)^2]}, \dots, e^{-j(\omega_{xk}M_x + \phi_{xk}M_x^2)}]^T$ denotes the manifold matrix of array \mathbf{x} , and \mathbf{A}_y is similarly defined. $\mathbf{n}_x(n)$ and $\mathbf{n}_y(n)$ represent the additive Gaussian noise vectors for the two ULAs.

Since ω_{xk} and ϕ_{xk} are only related to α_k and r_k , $\mathbf{a}(\omega_{xk}, \phi_{xk})$ is simplified into $\mathbf{a}_x(\alpha_k, r_k)$ in the following derivations and similarly, $\mathbf{a}(\omega_{yk}, \phi_{yk})$ is simplified into $\mathbf{a}_y(\beta_k, r_k)$, and the pair (ω_k, ϕ_k) can be determined by (α_k, β_k, r_k) based on the array signal model.

III. PROPOSED METHOD

A. Algorithm Description

In order to make full use of the spatial-temporal 2-D characteristics, $\mathbf{x}(n)$ and $\mathbf{y}(n)$ are divided into L frames according to the principle of maximum overlap in the time domain [21]. The l -th ($l = 1, 2, \dots, L$) frame data can be expressed as:

$$\begin{aligned} \mathbf{X}_l &= [\mathbf{x}(l), \mathbf{x}(l+1), \dots, \mathbf{x}(l+N-L)] \\ \mathbf{Y}_l &= [\mathbf{y}(l), \mathbf{y}(l+1), \dots, \mathbf{y}(l+N-L)] \end{aligned} \quad (8)$$

With the array signal model described in Section 2, the delay cross-correlation item of measured data $\mathbf{x}(n)$ and $\mathbf{y}(n)$ satisfies the following relationship

$$\begin{aligned} & r_{m_1, m_2}(l-1+L) \\ &= E\{x_{m_1}(n+l-1)y_{m_2}^*(n)\} \\ &= \sum_{k_1=1}^K [a_{x, m_1}(\alpha_{k_1}, r_{k_1}) a_{y, m_2}^*(\beta_{k_1}, r_{k_1}) \\ &\quad \times \mathbf{R}_{ss}(k_1, l-1+L)] + \delta(m_1)\delta(m_2)\delta(l-1)\sigma_w^2 \end{aligned} \quad (9)$$

Based on the rank reduction principle [9, 22], a new matrix can be constructed that is related to angle β :

$$\mathbf{D}(\beta) = \mathbf{C}^H(\beta)\mathbf{U}_n\mathbf{U}_n^H\mathbf{C}(\beta) \quad (25)$$

With (25), an estimator about β can be obtained:

$$\hat{\beta} = \arg \max_{\beta} \frac{1}{\det[\mathbf{D}(\beta)]} \quad (26)$$

With the same operation as (18), $\mathbf{a}_x(\alpha, r)$ can be decomposed into:

$$\mathbf{a}_x(\alpha, r) = \zeta_x(\alpha)\mathbf{v}_x(\alpha, r) \quad (27)$$

Rewrite equation (23) as:

$$\begin{aligned} & \tilde{\mathbf{a}}_{xy} \\ &= \begin{bmatrix} \mathbf{C}_1(\beta) & \\ & \mathbf{C}_2(\beta) \end{bmatrix} \begin{bmatrix} (\mathbf{v}_y^*(\beta, r) \otimes \mathbf{a}_x(\alpha, r)) \\ (\mathbf{v}_y(\beta, r) \otimes \mathbf{a}_x^*(\alpha, r)) \end{bmatrix} \\ &= \begin{bmatrix} \mathbf{C}_1(\beta) & \\ & \mathbf{C}_2(\beta) \end{bmatrix} \\ &\quad \times \begin{bmatrix} (\mathbf{I}_{M_y+1}\mathbf{v}_y^*(\beta, r) \otimes \zeta_x(\alpha)\mathbf{v}_x(\alpha, r)) \\ (\mathbf{I}_{M_y+1}\mathbf{v}_y(\beta, r) \otimes \zeta_x^*(\alpha)\mathbf{v}_x^*(\alpha, r)) \end{bmatrix} \\ &= \begin{bmatrix} \mathbf{C}_1(\beta) & \\ & \mathbf{C}_2(\beta) \end{bmatrix} \\ &\quad \times \begin{bmatrix} (\mathbf{I}_{M_y+1} \otimes \zeta_x(\alpha))(\mathbf{v}_y^*(\beta, r) \otimes \mathbf{v}_x(\alpha, r)) \\ (\mathbf{I}_{M_y+1} \otimes \zeta_x^*(\alpha))(\mathbf{v}_y(\beta, r) \otimes \mathbf{v}_x^*(\alpha, r)) \end{bmatrix} \\ &= \begin{bmatrix} \mathbf{C}_1(\beta) & \\ & \mathbf{C}_2(\beta) \end{bmatrix} \begin{bmatrix} \mathbf{E}_1(\alpha)(\mathbf{v}_y^*(\beta, r) \otimes \mathbf{v}_x(\alpha, r)) \\ \mathbf{E}_2(\alpha)(\mathbf{v}_y(\beta, r) \otimes \mathbf{v}_x^*(\alpha, r)) \end{bmatrix} \\ &= \begin{bmatrix} \mathbf{C}_1(\beta) & \\ & \mathbf{C}_2(\beta) \end{bmatrix} \begin{bmatrix} \mathbf{E}_1(\alpha) & \\ & \mathbf{E}_2(\alpha) \end{bmatrix} \\ &\quad \times \begin{bmatrix} (\mathbf{v}_y^*(\beta, r) \otimes \mathbf{v}_x(\alpha, r)) \\ (\mathbf{v}_y(\beta, r) \otimes \mathbf{v}_x^*(\alpha, r)) \end{bmatrix} \end{aligned} \quad (28)$$

where $\zeta_x(\alpha) \in \mathbb{C}^{N_x \times (M_x+1)}$, $\mathbf{E}_1(\alpha) = \mathbf{I}_{M_y+1} \otimes \zeta_x(\alpha)$ and $\mathbf{E}_2(\alpha) = \mathbf{I}_{M_y+1} \otimes \zeta_x^*(\alpha)$, all of which contain only the angle α information of the source, while $\mathbf{v}_x(\alpha, r) \in \mathbb{C}^{(M_x+1) \times 1}$ contains both the angle α and range information. Then, we define $\mathbf{E}(\alpha)$ that is only related to α :

$$\mathbf{E}(\alpha) = \begin{bmatrix} \mathbf{E}_1(\alpha) & \\ & \mathbf{E}_2(\alpha) \end{bmatrix} \quad (29)$$

Based on (29), another matrix related to both angle α and β can be constructed:

$$\mathbf{F}(\beta, \alpha) = \mathbf{E}^H(\alpha)\mathbf{C}^H(\beta)\mathbf{U}_n\mathbf{U}_n^H\mathbf{C}(\beta)\mathbf{E}(\alpha). \quad (30)$$

Substituting the estimated parameter $\hat{\beta}$ into $\mathbf{F}(\hat{\beta}, \alpha)$, another estimator in regard to the angle parameter $\hat{\alpha}$ can be obtained:

$$\hat{\alpha} = \arg \max_{\alpha} \frac{1}{\det[\mathbf{F}(\hat{\beta}, \alpha)]} \quad (31)$$

After obtaining the angle parameters of NF sources according to (26) and (31), substitute $\hat{\alpha}, \hat{\beta}$ into the classic MUSIC spectral function to construct the spectral peak search function about the range parameter r as follows:

$$\hat{r}_k = \arg \max_r f(\hat{\alpha}_k, \hat{\beta}_k, r) = \frac{1}{\tilde{\mathbf{a}}_{xy}^H(\hat{\alpha}, \hat{\beta}, r)\mathbf{U}_n\mathbf{U}_n^H\tilde{\mathbf{a}}_{xy}(\hat{\alpha}, \hat{\beta}, r)} \quad (32)$$

TABLE I
SUMMARY OF THE PROPOSED METHOD.

Input: N snapshots of the two ULA output vectors: $\{\mathbf{x}(t), \mathbf{y}(t)\}_{n=1}^N$.
Output: 2-D DOA and range estimates of NF signals: $\hat{\alpha}_k, \hat{\beta}_k$ and \hat{r}_k .
Step 1 Construct the conjugate augmented cross-correlation matrix $\tilde{\mathbf{R}}_{xy}$ with (11) and (14).
Step 2 Estimate and perform subspace decomposition on $\tilde{\mathbf{R}}$ to get \mathbf{U}_n .
Step 3 Construct and search through $\mathbf{D}(\beta)$ to obtain angles β_k with (26).
Step 4 Construct and search through $\mathbf{F}(\hat{\beta}, \alpha)$ to obtain angles α_k with (31).
Step 5 Construct and search through $f(\hat{\alpha}, \hat{\beta}, r)$ to obtain ranges r_k with (32).

At this point, the paired 2-D DOA and range parameters can be automatically obtained without any additional operation. The proposed method is summarized in Table I.

Remark 1: As several 1-D spatial spectrum searching procedures are required in the proposed method, the computationally efficient root-MUSIC method [23] can be applied to estimate the 2-D DOA and range parameters to reduce the complexity. As for the ESPRIT method [24], we have to construct some rotation invariant matrices that can not be easily achieved in this method.

Remark 2: The advantage of the proposed method is clarified as follows: 1) The proposed method employs the conjugate symmetry property of signal autocorrelation for different time delays to construct a conjugate augmented spatial-temporal cross correlation matrix; 2) three 1-D MUSIC-type searches are constructed, based on the properties of the Khatri-Rao product on the extended steering vector, which avoids the usual M-D search; 3) the proposed method can realize automatic pairing of multiple parameters associated with each source and it also works in the underdetermined case, as opposed to two existing representative algorithms [13, 15]; 4) the proposed method provides satisfactory estimation performance for both the DOA and range parameters in both low signal-to-noise ratio (SNR) and small number of snapshots conditions.

B. Discussion

1) Maximum Number of Distinguishable Sources

We first analyze (25) about the spectral function of β . $\mathbf{C}^H(\beta)\mathbf{U}_n \in \mathbb{C}^{2N_x(M_y+1) \times (2N_xN_y-K)}$ has full row rank, so we have

$$\begin{aligned} 2N_x(M_y+1) &\leq 2N_xN_y - K \Rightarrow \\ K &\leq 2N_x(N_y - M_y - 1) = N_x(N_y - 1) \end{aligned} \quad (33)$$

From (33), it can be seen that if β is to be correctly estimated, the upper limit of K is $N_x(N_y - 1)$, i.e., the number of sources must not be greater than $N_x(N_y - 1)$. In the same way, we analyze the spectral functions of α and r , namely (31) and (32), and can also obtain an upper limit for K . It is easy to see that these two upper limits are both higher than the value in (33), so it is omitted here.

Next, construct another delay cross-correlation function $r_{m_1, m_2}(l-1+L) = E\{y_{m_2}(n+l-1)x_{m_1}^*(n)\}$, and then the spectrum search function will be firstly constructed related to α , whose function form is the same as in (25), i.e.

$$\mathbf{D}(\alpha) = \mathbf{C}^H(\alpha)\mathbf{U}_n\mathbf{U}_n^H\mathbf{C}(\alpha) \quad (34)$$

where $\mathbf{C}^H(\alpha)\mathbf{U}_n \in \mathbb{C}^{2N_y(M_x+1) \times (2N_yN_x-K)}$. Since $\mathbf{C}^H(\alpha)\mathbf{U}_n$ is of full row rank, we have

$$\begin{aligned} 2N_y(M_x+1) &\leq 2N_yN_x - K \Rightarrow \\ K &\leq 2N_y(N_x - M_x - 1) = N_y(N_x - 1) \end{aligned} \quad (35)$$

Combining (33) and (35) together, it can be concluded that the proposed algorithm can detect at most $\min\{N_x(N_y-1), N_y(N_x-1)\}$ targets.

2) Computational Complexity

For computational complexity, we mainly consider the following parts: construction of the expansion matrices, EVD implementation and MUSIC spectral search. The method in [15] constructs one $N_x \times N_x$, one $N_y \times N_y$, one $(4M_y+1) \times (4M_y+1)$ and one $(4M_x+1) \times (4M_x+1)$ matrices, and implements their EVDs, so it has a complexity of $O\left\{9(N_x^2+N_y^2)N+9(4M_x+1)^2N+9(4M_y+1)^2N+4/3(N_x^3+N_y^3)+4/3(4M_x+1)^3+4/3(4M_y+1)^3+\pi N_x^2/\Delta\theta_\alpha+\pi N_y^2/\Delta\theta_\beta\right\}$, where $\Delta\theta_\alpha$ and $\Delta\theta_\beta$ are the search intervals for α and β , respectively. With similar analysis, the complexity of the method in [13] is $O\left\{(N_x^2+N_y^2)N+(M_x+2)^2M_x+(M_y+2)^2M_y+4/3(N_x^3+N_y^3)+4/3(M_x+2)^3+4/3(M_y+2)^3+\pi(M_x+2)^2+\pi(M_y+2)^2/\Delta\theta_\beta+Ran \cdot K \cdot (N_x^2+N_y^2)/\Delta r\right\}/\Delta\theta_\alpha$, where $Ran = 2D^2/\lambda - 0.62(D^2/\lambda)^{1/2}$ (D denotes the array aperture), and Δr is the search interval for r . However, the proposed algorithm constructs one $2N_xN_y \times (2L-1)$ matrix and then implements its EVD, followed by three 1-D searches. Therefore, the proposed algorithm has a complexity of $O\left\{N_xN_y(N-L+1)(2L-1)+(2N_xN_y)^2(2L-1)+4/3(2N_xN_y)^3+\pi N_x(N_y+1)(2N_xN_y)^2/\Delta\theta_\beta+\pi K \cdot (N_x+1)(N_y+1)^2N_x(N_xN_y)/\Delta\theta_\alpha+Ran \cdot K(2N_xN_y)^2/\Delta r\right\}$, which is higher than those of [13] and [15].

IV. CRAMER-RAO LOWER BOUND

In this section, we analyze the stochastic Cramer-Rao lower bound (CRB), which is an estimation benchmark for the variance of unbiased estimators. Under the stochastic assumption, a closed-form expression of the stochastic CRB is derived for both 2-D DOA and range parameters of NF sources, which is summarized in the following.

By concatenating the received data of the two ULA arrays in (8), namely,

$$\mathbf{Z}_l = \begin{bmatrix} \mathbf{X}_l \\ \mathbf{Y}_l \end{bmatrix}, \quad (36)$$

the time delays covariance matrix of \mathbf{Z}_l can be calculated as follows,

$$\tilde{\mathbf{R}}_{l_1} = \mathbf{Z}_{l+l_1-L}\mathbf{Z}_l^H. \quad (37)$$

Then, define a vector of unknown parameters as $\Phi = [\Omega^T \ \rho^T \ \sigma_w^2]^T$, $\Omega = [\alpha \ \beta \ \mathbf{r}]^T$ with $\alpha = [\theta_1, \theta_2, \dots, \theta_K]^T$, $\beta = [\beta_1, \beta_2, \dots, \beta_K]^T$, $\mathbf{r} = [r_1, r_2, \dots, r_K]^T$, and $\rho = [\rho_1, \rho_2, \dots, \rho_{2L-1}]^T$ is a $K(2L-1) \times 1$ vector with each element ρ_{l_1} represented as $\rho_{l_1} = [\mathbf{P}_{l_1}(1,1), \dots, \mathbf{P}_{l_1}(k,k), \dots, \mathbf{P}_{l_1}(K,K)]$, where $\mathbf{P}_{l_1} = \mathbf{S}_{l_1-L+l_1}\mathbf{S}_{l_1}^H$.

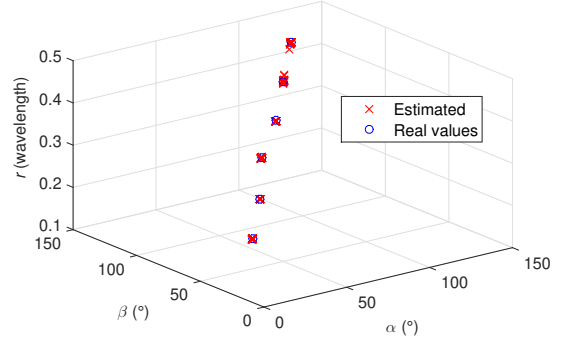


Fig. 2. 3-D scattergram of six NF sources.

According to the Slepian-Bangs formulation [25, 26], the Fisher information matrix (FIM) of Φ , which is based on the time delays covariance matrices $\tilde{\mathbf{R}}_1, \tilde{\mathbf{R}}_2, \dots, \tilde{\mathbf{R}}_{2L-1}$, is given by

$$\mathbf{FIM}_{i,j} = \sum_{l_1=1}^{2L-1} (N+L-1)tr \left(\frac{\partial \tilde{\mathbf{R}}_{l_1}}{\partial \Phi_i} \tilde{\mathbf{R}}_{l_1}^{-1} \frac{\partial \tilde{\mathbf{R}}_{l_1}}{\partial \Phi_j} \tilde{\mathbf{R}}_{l_1}^{-1} \right). \quad (38)$$

By vectorizing the matrix $\tilde{\mathbf{R}}_{l_1}$, we have

$$\begin{aligned} \tilde{\mathbf{r}}_{l_1} &= \text{vec}(\tilde{\mathbf{R}}_{l_1}) \\ &= \left(\begin{bmatrix} \mathbf{A}_x^*(\alpha, r) \\ \mathbf{A}_y^*(\beta, r) \end{bmatrix} \right) \odot \left(\begin{bmatrix} \mathbf{A}_x(\alpha, r) \\ \mathbf{A}_y(\beta, r) \end{bmatrix} \right) \mathbf{P}_{l_1} + \sigma_w^2 \text{vec}(\mathbf{R}_{w_{l_1}}) \end{aligned} \quad (39)$$

where

$$\mathbf{R}_{w_{l_1}} = \begin{cases} \mathbf{I}_{M_x M_y}, & l_1 = L \\ \mathbf{0}, & l_1 \neq L \end{cases} \quad (40)$$

With (39), (38) can be rewritten in a compact matrix form as follows,

$$\mathbf{FIM} = \left(\frac{\partial \tilde{\mathbf{r}}}{\partial \Phi^T} \right)^H \mathbf{C}_{\tilde{\mathbf{r}}}^{-1} \left(\frac{\partial \tilde{\mathbf{r}}}{\partial \Phi^T} \right) \quad (41)$$

where $\tilde{\mathbf{r}} = [\tilde{\mathbf{r}}_1^T, \dots, \tilde{\mathbf{r}}_{2L-1}^T]^T$, and $\mathbf{C}_{\tilde{\mathbf{r}}} = \text{blkdiag}\{\mathbf{C}_{\tilde{\mathbf{r}}_1}, \dots, \mathbf{C}_{\tilde{\mathbf{r}}_{2L-1}}\}$ with each element $\mathbf{C}_{\tilde{\mathbf{r}}_{l_1}} = \frac{1}{N+L-1} \tilde{\mathbf{R}}_{l_1}^T \otimes \tilde{\mathbf{R}}_{l_1}$.

Next, we partition $\frac{\partial \tilde{\mathbf{r}}}{\partial \Phi^T}$ as

$$\frac{\partial \tilde{\mathbf{r}}}{\partial \Phi^T} = [\tilde{\mathbf{D}} \quad \tilde{\mathbf{\Lambda}}] \quad (42)$$

where $\tilde{\mathbf{D}} = [\tilde{\mathbf{D}}_1^T, \dots, \tilde{\mathbf{D}}_{2L-1}^T]^T$ and $\tilde{\mathbf{\Lambda}} = [\tilde{\mathbf{\Lambda}}_1^T, \dots, \tilde{\mathbf{\Lambda}}_{2L-1}^T]^T$ with the element denoted as $\tilde{\mathbf{D}}_{l_1} = (\frac{\partial \tilde{\mathbf{r}}_{l_1}}{\partial \alpha}, \frac{\partial \tilde{\mathbf{r}}_{l_1}}{\partial \beta}, \frac{\partial \tilde{\mathbf{r}}_{l_1}}{\partial r})$ and $\tilde{\mathbf{\Lambda}}_{l_1} = (\frac{\partial \tilde{\mathbf{r}}_{l_1}}{\partial \rho}, \frac{\partial \tilde{\mathbf{r}}_{l_1}}{\partial \sigma_w^2})$.

By left-multiplying matrix $\mathbf{C}_{\tilde{\mathbf{r}}}^{-\frac{1}{2}}$ with $\tilde{\mathbf{D}}$ and $\tilde{\mathbf{\Lambda}}$ in (42), we obtain $\tilde{\tilde{\mathbf{D}}} = \mathbf{C}_{\tilde{\mathbf{r}}}^{-\frac{1}{2}} \tilde{\mathbf{D}}$ and $\tilde{\tilde{\mathbf{\Lambda}}} = \mathbf{C}_{\tilde{\mathbf{r}}}^{-\frac{1}{2}} \tilde{\mathbf{\Lambda}}$. Further, (41) can be changed to

$$\mathbf{FIM} = \begin{bmatrix} \tilde{\tilde{\mathbf{D}}}^H & \tilde{\tilde{\mathbf{D}}} & \tilde{\tilde{\mathbf{D}}}^H & \tilde{\tilde{\mathbf{\Lambda}}} \\ \tilde{\tilde{\mathbf{D}}} & \tilde{\tilde{\mathbf{D}}} & \tilde{\tilde{\mathbf{D}}} & \tilde{\tilde{\mathbf{\Lambda}}} \\ \tilde{\tilde{\mathbf{D}}}^H & \tilde{\tilde{\mathbf{D}}} & \tilde{\tilde{\mathbf{D}}}^H & \tilde{\tilde{\mathbf{\Lambda}}} \\ \tilde{\tilde{\mathbf{\Lambda}}} & \tilde{\tilde{\mathbf{\Lambda}}} & \tilde{\tilde{\mathbf{\Lambda}}} & \tilde{\tilde{\mathbf{\Lambda}}} \end{bmatrix} \quad (43)$$

Finally, the CRB of the parameter of interest Ω , namely the 2-D DOAs and ranges can be obtained as

$$\text{CRB}_{\Omega} = \tilde{\tilde{\mathbf{D}}}^H \Pi_{\tilde{\tilde{\mathbf{\Lambda}}}} \tilde{\tilde{\mathbf{D}}} \quad (44)$$

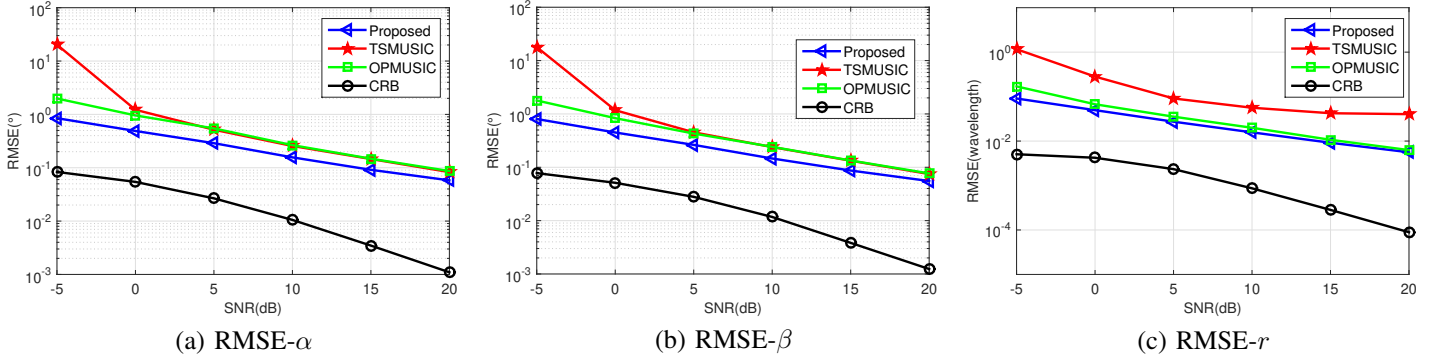


Fig. 3. RMSE versus SNR in Example 2 ($N = 400$, $L = 50$, $K=2$, $(50^\circ, 60^\circ, 0.8\lambda)$ and $(90^\circ, 100^\circ, 1.3\lambda)$).

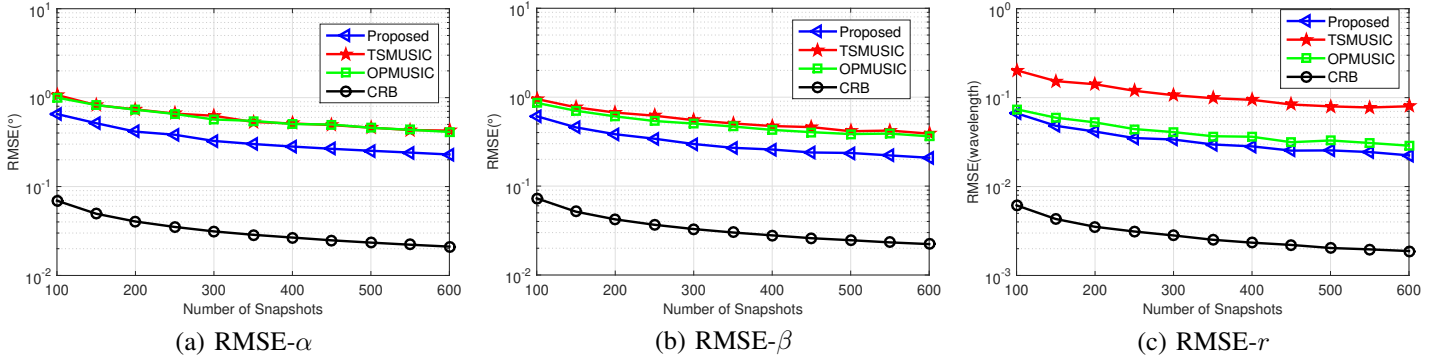


Fig. 4. RMSE versus snapshots in Example 3 (SNR = 5dB, $L = 50$, $K = 2$).

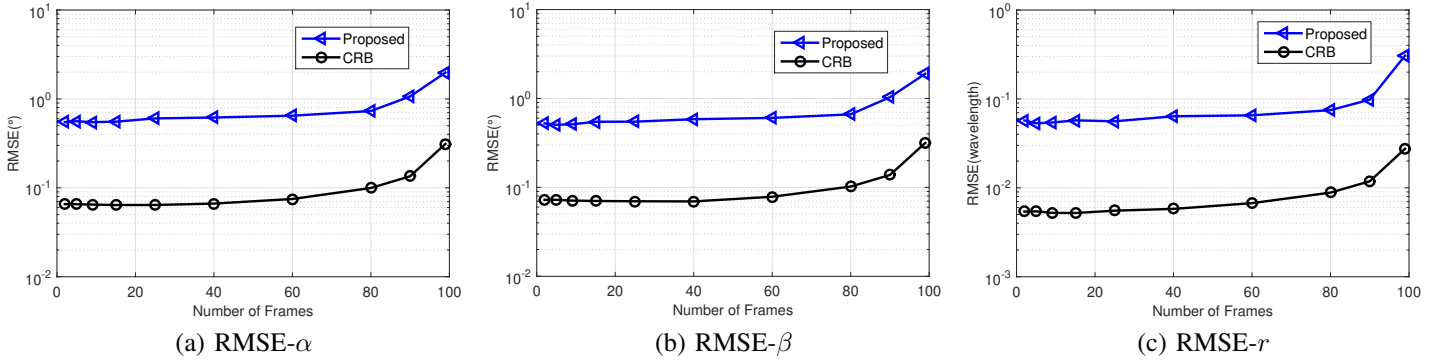


Fig. 5. RMSE versus frames in Example 4 (SNR = 5dB, $N = 100$, $K=2$).

where $\Pi_{\tilde{\Lambda}}^{\perp} = \mathbf{I} - \tilde{\Lambda}(\tilde{\Lambda}^H \tilde{\Lambda})^{-1} \tilde{\Lambda}^H$.

V. SIMULATION RESULTS

In this section, simulation results are provided to demonstrate the performance of the proposed algorithm, in comparison with OPMUSIC [13] and TSMUSIC [15], where $d = \lambda/4$, all NF signals are of equal power σ_s^2 , and the SNR is defined as $10\log_{10}(\sigma_s^2/\sigma_w^2)$. Define the estimation root-mean-square error (RMSE) from V Monte Carlo trials as:

$$RMSE = \sqrt{\frac{1}{KV} \sum_{v=1}^V \sum_{k=1}^K (\hat{x}_k^{(v)} - x_k)^2}. \quad (45)$$

Example 1: Test for maximum number of distinguishable sources - There are six uncorrelated NF sources from $(20^\circ, 35^\circ, 0.2\lambda)$, $(40^\circ, 55^\circ, 0.25\lambda)$, $(60^\circ, 80^\circ, 0.3\lambda)$, $(80^\circ, 95^\circ, 0.35\lambda)$, $(100^\circ, 115^\circ, 0.4\lambda)$, and $(120^\circ, 135^\circ, 0.45\lambda)$ impinging onto a symmetric cross array with $M_x = M_y = 1$, i.e., each ULA has only 3 sensors and the total number of elements of the cross array is 5. The SNR, the number of snapshots N , the number of frames L and Monte Carlo trials are set to be 30dB, 1000, 100 and 50, respectively. The estimation result is shown in Fig. 2, where it can be seen that all the six NF sources have been identified and the 3-D parameters can be paired correctly, showing that the proposed

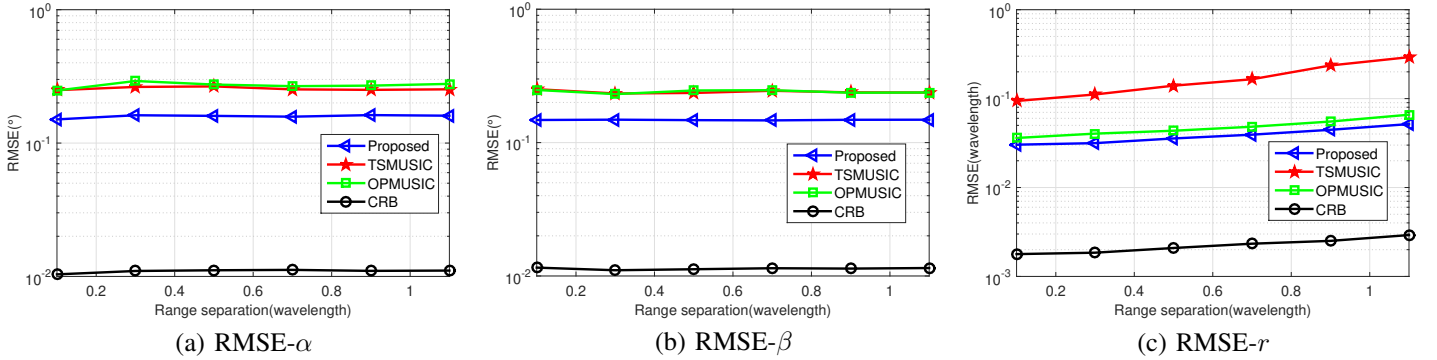


Fig. 6. RMSE versus frames in Example 5 (SNR = 10dB, $K=2$, $(50^\circ, 60^\circ, (0.8 + \Delta\lambda)\lambda)$ and $(90^\circ, 100^\circ, 1.9\lambda)$).

algorithm is working effectively for the underdetermined case.

Example 2: RMSE versus SNR - The performance of the proposed algorithm is studied with respect to SNR. There are three uncorrelated NF sources impinging onto a symmetric cross array with $M_x = M_y = 2$. The number of snapshots N , frames L and Monte Carlo trials are set to be 400, 50 and 500, respectively. From Fig. 3, we can see that the estimation performance of the proposed algorithm is better than the other two algorithms, especially for low SNR regions. This is because the proposed method makes better use of space-time information of the incident signals than the other methods.

Example 3: RMSE versus Snapshots - In this example, the performance of the proposed algorithm is studied with respect to the number of snapshots. The number of signals and the number of array elements are the same as in Example 2. The SNR is set to 5dB. The number of frames L is 50. The results are provided in Fig. 4, from which we can see that the RMSE of all algorithms decreases with the increase of number of snapshots, and the estimation accuracy of the proposed method is better than those of the other methods in both 2-D DOA and range parameters.

Example 4: RMSE versus Frames - In this example, we investigate the effect of different number of frames on the estimation performance of the proposed algorithm. The simulation parameter settings are the same as in Example 3, except for the number of frames and snapshots. The number of snapshots N is 100 and the number of frames L varies from 2 to 99. As shown in Fig. 5, when L becomes too large ($L=99$), little data is available in each frame which has a significant detrimental effect on subsequent subspace angle estimation accuracy, leading to a sharp increase in the RMSE.

Example 5: RMSE versus Range separation - In the last set of simulations, the parameter settings are the same as Example 1, except that the SNR is fixed at 15 dB, and the range separation $\Delta\lambda$ of the first source varies from 0.1λ to 1.1λ . The RMSE versus the range separation is shown in Fig. 6. It can be seen that the 2-D angle estimates in all three algorithms are insensitive to range separation, except for the range estimates. In addition, it can be seen that the range estimate has good accuracy for small range separations, as the first source is closer to the array, which is consistent with the analysis in [15].

VI. CONCLUSIONS

In this work, a new localization method for NF sources has been proposed using a cross array. It can realize 3-D parameter estimation for the underdetermined case with automatic pairing, and as it does not require simultaneous multi-dimensional search, it has a low computational complexity. In addition, the stochastic CRB was derived for the circumstance with different time delays as a performance benchmark. As demonstrated by computer simulations, it has outperformed two existing representative algorithms.

REFERENCES

- [1] Ting Shu, Jin He, and Veerendra Dakulagi, "3-D near-field source localization using a spatially spread acoustic vector sensor," *IEEE Transactions on Aerospace and Electronic Systems*, pp. 1–1, 2021.
- [2] Zhi Zheng, Mingcheng Fu, Wen-Qin Wang, and Hing Cheung So, "Symmetric displaced coprime array configurations for mixed near- and far-field source localization," *IEEE Transactions on Antennas and Propagation*, vol. 69, no. 1, pp. 465–477, 2021.
- [3] Liana Khamidullina, Ivan Podkurkov, and Martin Haardt, "Conditional and unconditional cram-rao bounds for near-field localization in bistatic MIMO radar systems," *IEEE Transactions on Signal Processing*, vol. 69, pp. 3220–3234, 2021.
- [4] Weiliang Zuo, Jingmin Xin, Wenyi Liu, Nanning Zheng, Hiromitsu Ohmori, and Akira Sano, "Localization of near-field sources based on linear prediction and oblique projection operator," *IEEE Transactions on Signal Processing*, vol. 67, no. 2, pp. 415–430, 2019.
- [5] Junpeng Shi, Fangqing Wen, and Tianpeng Liu, "Nested MIMO radar: Coarrays, tensor modeling, and angle estimation," *IEEE Transactions on Aerospace and Electronic Systems*, vol. 57, no. 1, pp. 573–585, 2021.
- [6] Riheng Wu, Mei Wang, and Zhenhai Zhang, "Computationally efficient DOA and carrier estimation for coherent signal using single snapshot and its time-delay replications," *IEEE Transactions on Aerospace and Electronic Systems*, vol. 57, no. 4, pp. 2469–2480, 2021.
- [7] Zhi Zheng, Yixiao Huang, Wen-Qin Wang, and Hing Cheung So, "Augmented covariance matrix reconstruction for DOA estimation using difference coarray," *IEEE Transactions on Signal Processing*, vol. 69, pp. 5345–5358, 2021.
- [8] Qisen Wang, Hua Yu, Jie Li, Fei Ji, and Fangjiong Chen, "Sparse bayesian learning using generalized double pareto prior for DOA estimation," *IEEE Signal Processing Letters*, vol. 28, pp. 1744–1748, 2021.
- [9] Hua Chen, Weifeng Wang, and Wei Liu, "Joint DOA, range, and polarization estimation for rectilinear sources with a cold array," *IEEE Wireless Communications Letters*, vol. 8, no. 5, pp. 1398–1401, 2019.
- [10] A.L. Swindlehurst and T. Kailath, "Passive direction-of-arrival and range estimation for near-field sources," in *Fourth Annual ASSP Workshop on Spectrum Estimation and Modeling*, 1988, pp. 123–128.
- [11] Y.-D. Huang and M. Barkat, "Near-field multiple source localization by passive sensor array," *IEEE Transactions on Antennas and Propagation*, vol. 39, no. 7, pp. 968–975, 1991.

- [12] A.J. Weiss and B. Friedlander, "Range and bearing estimation using polynomial rooting," *IEEE Journal of Oceanic Engineering*, vol. 18, no. 2, pp. 130–137, 1993.
- [13] Jin He, M. N. S. Swamy, and M. Omair Ahmad, "Efficient application of music algorithm under the coexistence of far-field and near-field sources," *IEEE Transactions on Signal Processing*, vol. 60, no. 4, pp. 2066–2070, 2012.
- [14] Xiaofei Zhang, Weiyang Chen, Wang Zheng, Zhongxi Xia, and Yunfei Wang, "Localization of near-field sources: A reduced-dimension MUSIC algorithm," *IEEE Communications Letters*, vol. 22, no. 7, pp. 1422–1425, 2018.
- [15] Junli Liang and Ding Liu, "Passive localization of mixed near-field and far-field sources using two-stage music algorithm," *IEEE Transactions on Signal Processing*, vol. 58, no. 1, pp. 108–120, 2010.
- [16] Ke Deng and Qinye Yin, "Closed form parameters estimation for 3-D near field sources," in *2006 IEEE International Conference on Acoustics Speech and Signal Processing Proceedings*, 2006, vol. 4, pp. IV–IV.
- [17] K. Abed-Meraim and Y. Hua, "3-D near field source localization using second order statistics," in *Conference Record of the Thirty-First Asilomar Conference on Signals, Systems and Computers (Cat. No.97CB36136)*, 1997, vol. 2, pp. 1307–1311 vol.2.
- [18] Xiaohuan Wu and Wei-Ping Zhu, "Single far-field or near-field source localization with sparse or uniform cross array," *IEEE Transactions on Vehicular Technology*, vol. 69, no. 8, pp. 9135–9139, 2020.
- [19] Raghu N. Challa and Sanyogita Shamsunder, "Passive near-field localization of multiple non-gaussian sources in 3-D using cumulants," *Signal Processing*, vol. 65, no. 1, pp. 39–53, 1998.
- [20] Xiaohuan Wu and Jun Yan, "3-D mixed far-field and near-field sources localization with cross array," *IEEE Transactions on Vehicular Technology*, vol. 69, no. 6, pp. 6833–6837, 2020.
- [21] Yang-Yang Dong, Chun-xi Dong, Zhi-bo Shen, and Guo-qing Zhao, "Conjugate augmented spatial temporal technique for 2-D DOA estimation with l-shaped array," *IEEE Antennas and Wireless Propagation Letters*, vol. 14, pp. 1622–1625, 2015.
- [22] Hua Chen, Wei Liu, Wei-Ping Zhu, and M.N.S. Swamy, "Noncircularity-based localization for mixed near-field and far-field sources with unknown mutual coupling," in *2018 IEEE International Conference on Acoustics, Speech and Signal Processing (ICASSP)*, 2018, pp. 3236–3240.
- [23] B.D. Rao and K.V.S. Hari, "Performance analysis of root-MUSIC," *IEEE Transactions on Acoustics, Speech, and Signal Processing*, vol. 37, no. 12, pp. 1939–1949, 1989.
- [24] R. Roy and T. Kailath, "ESPRIT-estimation of signal parameters via rotational invariance techniques," *IEEE Transactions on Acoustics, Speech, and Signal Processing*, vol. 37, no. 7, pp. 984–995, 1989.
- [25] P. Stoica, E.G. Larsson, and A.B. Gershman, "The stochastic CRB for array processing: a textbook derivation," *IEEE Signal Processing Letters*, vol. 8, no. 5, pp. 148–150, 2001.
- [26] Yibao Liang, Wei Liu, Qing Shen, Wei Cui, and Siliang Wu, "A review of closed-form Cramer-Rao bounds for DOA estimation in the presence of gaussian noise under a unified framework," *IEEE Access*, vol. 8, pp. 175101–175124, 2020.